

See discussions, stats, and author profiles for this publication at: <https://www.researchgate.net/publication/24423016>

First Direct Imaging of Electrolyte-Induced Deswelling Behavior of pH-Responsive Microgels in Aqueous Media Using Scanning Transmission X-ray Microscopy

ARTICLE in LANGMUIR · APRIL 2009

Impact Factor: 4.46 · DOI: 10.1021/la804212y · Source: PubMed

CITATIONS

29

READS

60

5 AUTHORS, INCLUDING:



Syuji Fujii

Osaka Institute of Technology

160 PUBLICATIONS 2,755 CITATIONS

SEE PROFILE



Damien Dupin

IK4-CIDETEC

37 PUBLICATIONS 806 CITATIONS

SEE PROFILE



Tohru Araki

Diamond Light Source

86 PUBLICATIONS 2,727 CITATIONS

SEE PROFILE



Steven P Armes

The University of Sheffield

612 PUBLICATIONS 27,316 CITATIONS

SEE PROFILE

First Direct Imaging of Electrolyte-Induced Deswelling Behavior of pH-Responsive Microgels in Aqueous Media Using Scanning Transmission X-ray Microscopy

Syuji Fujii,^{*,†} Damien Dupin,[‡] Tohru Araki,^{*,§,||} Steven P. Armes,[‡] and Harald Ade[§]

Department of Applied Chemistry, Faculty of Engineering, Osaka Institute of Technology, 5-16-1 Ohmiya, Asahi-ku, Osaka 535-8585, Japan, Department of Chemistry, Dainton Building, The University of Sheffield, Brook Hill, Sheffield, South Yorkshire S3 7HF, U.K., and Department of Physics, North Carolina State University, Raleigh, North Carolina 27695

Received December 22, 2008. Revised Manuscript Received January 15, 2009

Lightly cross-linked sterically stabilized poly(2-vinylpyridine) latexes exhibit pH-responsive behavior, undergoing a latex-to-microgel transition below pH 4.1 as a result of protonation of the pyridine pendent groups. We have examined both the latex and microgel states of such particles directly in aqueous solution using scanning transmission X-ray microscopy (STXM). Moreover, near-edge X-ray absorption fine structure (NEXAFS) spectroscopy studies confirm that the nitrogen atoms of the microgel particles are fully protonated at low pH. The addition of salt causes partial deswelling of these microgel particles, but spectroscopic analysis confirms the retention of their cationic character. This is the first direct visualization of the effect of electrolyte screening on microgel dimensions in aqueous solution. In each case, the observed particle dimensions are consistent with dynamic light scattering characterization, especially when polydispersity effects are taken into consideration.

Introduction

Aqueous stimuli-responsive hydrogel nanoparticles (microgels) have received increasing attention¹ because of their potential applications in various fields, including drug delivery,² chemical separations,³ sensors,⁴ dynamically tunable microlenses,⁵ templates for inorganic nanoparticle synthesis,⁶ water purification,⁷ viscosity modifiers,⁸ and “smart” particulate emulsifiers.⁹ Many examples of pH-responsive microgels have been reported over the past decade or so. These include (i) methacrylic acid-based alkali-swellable latexes;^{10,11} (ii) *N*-isopropylacrylamide-based copolymer microgels containing either acidic or basic comono-

mers;^{12–14} and (iii) acid-swellable latexes based on basic monomers such as 4-vinylpyridine, 2-vinylpyridine (2VP), or tertiary amine methacrylates such as 2-(diethylamino)ethyl methacrylate or 2-(diisopropylamino)ethyl methacrylate.^{15–17} It is well known that the degree of swelling of these pH-responsive aqueous microgels is influenced by the presence of electrolytes, which should change the properties of the microgel dispersions such as viscosity and turbidity. The direct characterization of (de)swelling behavior of the microgel induced by changes in pH and/or electrolyte concentration in the aqueous solution is important in understanding their colloidal behavior. Dynamic light scattering (DLS) is a convenient technique for measuring the degree of (de)swelling. However, swollen microgel diameters often approach or exceed 1 μm , which is close to the upper limit for DLS. Furthermore, this scattering technique can provide no morphological or spectroscopic information. There are several imaging techniques for colloidal particles dispersed in aqueous

* Corresponding authors. (S.F.) E-mail: s.fujii@chem.oit.ac.jp. (T.A.) E-mail: taraki@spring8 or jp/taraki@mosk.tytlabs.co.jp.

[†] Osaka Institute of Technology.

[‡] The University of Sheffield.

[§] North Carolina State University.

^{||} Current address: TOYOTA Central R&D Labs., Inc., Nagakute, Aichi 480-1192, Japan.

(1) (a) Murray, M. J.; Snowden, M. J. *Adv. Colloid Interface Sci.* **1995**, *54*, 73. (b) Saunders, B. R.; Vincent, B. *Adv. Colloid Interface Sci.* **1999**, *80*, 73. (c) Pelton, R. H. *Adv. Colloid Interface Sci.* **2000**, *85*, 1. (d) Kawaguchi, H. *Prog. Polym. Sci.* **2000**, *25*, 1171. (e) Lyon, L. A.; Debord, J. D.; Debord, S. B.; Jones, C. D.; McGrath, J. G.; Serpe, M. J. *J. Phys. Chem. B* **2004**, *108*, 19099.

(2) (a) Jeong, B.; Bae, Y. H.; Lee, D. S.; Kim, S. W. *Nature* **1997**, *388*, 860. (b) Hoffman, A. “Intelligent” Polymers. In *Controlled Drug Delivery: Challenges and Strategies*; Park, K., Ed.; American Chemical Society: Washington, DC, 1997; pp 485–498. (c) Nayak, S.; Lee, H.; Chmielewski, J.; Lyon, L. A. *J. Am. Chem. Soc.* **2004**, *126*, 10258. (d) Murthy, N.; Thng, Y. X.; Schuck, S.; Xu, M. C.; Fréchet, J. M. J. *J. Am. Chem. Soc.* **2002**, *124*, 12398.

(3) (a) Kawaguchi, H.; Fujimoto, K. *Bioseparation* **1998**, *7*, 253. (b) Umeno, D.; Kawasaki, M.; Maeda, M. *Bioconjugate Chem.* **1998**, *9*, 719.

(4) Holtz, J. H.; Asher, S. A. *Nature* **1997**, *389*, 829.

(5) (a) Kim, J.; Serpe, M. I.; Lyon, L. A. *J. Am. Chem. Soc.* **2004**, *126*, 9512. (b) Serpe, M. J.; Kim, J.; Lyon, L. A. *Adv. Mater.* **2004**, *16*, 184.

(6) (a) Zhang, J.; Xu, S.; Kumacheva, E. *J. Am. Chem. Soc.* **2004**, *126*, 7908. (b) Gorelikov, I.; Field, L. M.; Kumacheva, E. *J. Am. Chem. Soc.* **2004**, *126*, 15938. (c) Suzuki, D.; Kawaguchi, H. *Langmuir* **2005**, *21*, 8175.

(7) (a) Snowden, M. J.; Thomas, D.; Vincent, B. *Analyst* **1993**, *118*, 1367. (b) Morris, G. E.; Vincent, B.; Snowden, M. J. *Colloid Interface Sci.* **1997**, *190*, 198.

(8) Ole Kiminta, D. M.; Luckham, P. F.; Lenon, S. *Polymer* **1995**, *36*, 4827.

(9) (a) Fujii, S.; Read, E. S.; Armes, S. P.; Binks, B. P. *Adv. Mater.* **2005**, *17*, 1014. (b) Ngai, T.; Behrens, S. H.; Auweter, H. *Chem. Commun.* **2005**, *3*, 331. (c) Suzuki, D.; Tsuji, S.; Kawaguchi, H. *J. Am. Chem. Soc.* **2007**, *129*, 8088.

(10) (a) Tan, B. H.; Tam, K. C.; Lam, Y. C.; Tan, C. B. *Langmuir* **2005**, *21*, 4283. (b) Tan, B. H.; Tam, K. C.; Lam, Y. C.; Tan, C. B. *Adv. Colloid Interface Sci.* **2005**, *113*, 111. (c) Tan, B. H.; Ravi, P.; Tam, K. C. *Macromol. Rapid Commun.* **2006**, *27*, 522.

(11) (a) Rodriguez, B. E.; Wolfe, M. S.; Fryd, M. *Macromolecules* **1994**, *27*, 6642. (b) Saunders, B. R.; Crowther, H. M.; Vincent, B. *Macromolecules* **1997**, *30*, 482. (c) Tirtaatmadja, V.; Tam, K. C.; Jenkins, R. D. *Macromolecules* **1997**, *30*, 3271.

(12) (a) Bradley, M.; Ramos, J.; Vincent, B. *Langmuir* **2005**, *21*, 1209. (b) Nerapuri, V.; Keddie, J. L.; Vincent, B.; Bushnak, I. A. *Langmuir* **2006**, *22*, 5036. (c) Deng, Y.; Pelton, R. *Macromolecules* **1995**, *28*, 4617.

(13) (a) Gan, G.; Lyon, L. A. *J. Am. Chem. Soc.* **2001**, *123*, 7511. (b) Jones, C. D.; Lyon, L. A. *Macromolecules* **2003**, *36*, 1988. (c) Serpe, M. J.; Lyon, L. A. *Chem. Mater.* **2004**, *16*, 4373. (d) Kim, J.; Kayak, S.; Lyon, L. A. *J. Am. Chem. Soc.* **2005**, *127*, 9588.

(14) (a) Gorelikov, I.; Field, L. M.; Kumacheva, E. *J. Am. Chem. Soc.* **2004**, *126*, 15938. (b) Suzuki, D.; Kawaguchi, H. *Colloid Polym. Sci.* **2006**, *284*, 309. (c) Hoare, T.; Pelton, R. *Langmuir* **2004**, *20*, 282. (d) Hoare, T.; Pelton, R. *Langmuir* **2006**, *22*, 7342. (e) Hoare, T.; Pelton, R. *Macromolecules* **2004**, *37*, 2544. (f) Zhang, J.; Xu, S.; Kumacheva, E. *J. Am. Chem. Soc.* **2004**, *126*, 7908.

(15) Ma, G. H.; Fukutomi, T. *Macromolecules* **1992**, *25*, 1870.

(16) (a) Loxley, A.; Vincent, B. *Colloid Polym. Sci.* **1997**, *275*, 1108. (b) Atkin, R.; Bradley, M.; Vincent, B. *Soft Matter* **2005**, *1*, 160. (c) Dupin, D.; Fujii, S.; Armes, S. P.; Reeve, P.; Baxter, S. M. *Langmuir* **2006**, *22*, 3381.

(17) (a) U.S. Patent No. 4,170,685, 1979. (b) Mitsui Cyanamid KK, European Patent EP0385627, 1990. (c) Amalvy, J. I.; Wanless, E. J.; Michailidou, V.; Armes, S. P.; Duccini, Y. *Langmuir* **2004**, *20*, 8992.

media. Optical microscopy (OM) is useful for sizing relatively large particles in solution. However, because of the wavelength of visible light and other constraints, the effective OM resolution limit is approximately $1\ \mu\text{m}$. Moreover, it is very difficult to observe even micrometer-sized microgels directly because of the very small difference in refractive index between the swollen particles and the continuous phase. Confocal laser scanning microscopy (CLSM) is also a powerful technique for observing microgel particles in the wet state. However, this method also suffers from relatively low resolution, and the microgels must be fluorescently labeled, which may affect their (de)swelling properties. Recently, AFM was used to image hydrated microgel particles adsorbed on mica in aqueous solutions, thereby avoiding the gross structural changes that can occur upon drying. However, no spectroscopic information can be obtained with this technique.¹⁸

Scanning transmission X-ray microscopy (STXM) combines excellent compositional sensitivity via near-edge X-ray absorption fine structure (NEXAFS)¹⁹ spectroscopy with high spatial resolution and has been recently used to study a number of polymer systems.²⁰ The so-called “water window” ($E = 284\text{--}543\ \text{eV}$) corresponding to photon energies between the K-shell absorption edge of carbon and oxygen allows STXM characterization of fully hydrated organic samples such as biofilms²¹ and synthetic polymers.²² The polymer STXM²³ at beam line 5.3.2 of the Advanced Light Source used in this work provides images with better than 50 nm spatial resolution and a spectral resolution $E/\Delta E$ of more than 2000. Recently, we succeeded in direct imaging of submicrometer-sized, pH-responsive poly(4-vinylpyridine)/silica nanocomposite microgels while obtaining simultaneous spectroscopic information regarding their in situ chemical state (i.e., whether the polymer chains were protonated or deprotonated) by NEXAFS.²⁴ In contrast, the present study is focused on pH-responsive poly(2-vinylpyridine) (P2VP) latex/microgel particles.^{16c} The P2VP particles were synthesized in their latex form by emulsion polymerization of 2VP and divinylbenzene in the presence of monomethoxy-capped poly(ethylene glycol) methacrylate (PEGMA) macromonomer in aqueous solution: the PEGMA chains are grafted onto the outside of the latex particles and act as a steric stabilizer. Figure 1 illustrates the latex-to-microgel transition exhibited by these pH-responsive particles as a result of the protonation of the pyridine nitrogen atoms at low pH. After each pH cycle, the degree of microgel swelling observed at low pH was reduced: the background salt concentration inevitably increased after each pH cycle, which causes partial deswelling due to the salt-induced

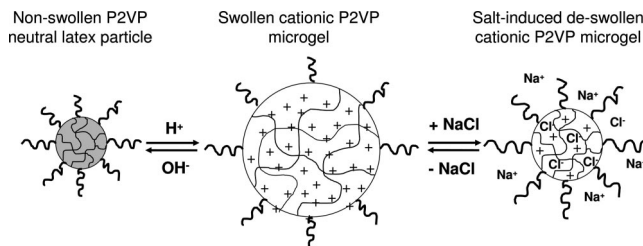


Figure 1. Schematic representation of the pH-responsive and salt-induced swelling and deswelling behaviors observed for sterically stabilized poly(2-vinylpyridine) (P2VP) microgel particles.

screening of the electrostatic repulsive forces between the cationic P2VP chains (Figure 1). The steric stabilization conferred by the chemically grafted PEGMA chains ensures that the P2VP particles are colloiddally stable even at relatively high salt concentrations, whereas merely charge-stabilized microgel particles tend to flocculate under such conditions. Herein we describe the first direct imaging and spectroscopic characterization of the pH- and electrolyte-induced (de)swelling behavior of microgel particles in aqueous solution using the STXM.

Experimental Section

Poly(2-vinylpyridine) Latex Synthesis via Emulsion Polymerization. This synthesis has been described in detail elsewhere.^{16c} Aliquat 336 surfactant (0.50 g, Aldrich) and the PEGMA stabilizer (1.0 g, Cognis Performance Chemicals, Hythe, U.K.) were dissolved in deionized water (38.5 g) in a 100 mL single-necked round-bottomed flask. A comonomer mixture of 2VP (4.95 g, Aldrich) and DVB (0.05 g, Fluka) was then added, causing the solution pH to increase to approximately 8.3. The flask was sealed with a rubber septum and the aqueous solution was degassed at ambient temperature using five vacuum/nitrogen cycles. The degassed solution was stirred at 250 rpm using a magnetic stirrer, heated to 60 °C with the aid of an oil bath, and then the aqueous azo initiator solution (0.05 g of α,α' -azodiisobutyramidine dihydrochloride (AIBA, 97%, Aldrich) dissolved in 4.95 g water) was injected after 20 min. The copolymerizing solution turned milky white within 10 min, and stirring was continued for 24 h at 60 °C.

Purification. The P2VP latex particles were centrifuged at 8000 rpm for 40 min, followed by careful decantation of the supernatant, replacement with fresh water, and redispersion of the sedimented particles with the aid of an ultrasonic bath. This protocol was used to remove residual 2VP monomer, excess Aliquat 336 surfactant, and nongrafted PEGMA stabilizer. The extent of latex purification was assessed by measuring the surface tension of the serum or supernatant, respectively; purification was continued until this surface tension was close to that of pure water ($72\ \text{mN m}^{-1}$).

Field Emission Scanning Electron Microscopy. SEM studies were carried out using a FEG-SEM Inspect F instrument operating at 20 kV. Dried samples were placed on an aluminum stub and sputter-coated with gold to minimize sample-charging problems.

Dynamic Light Scattering. Hydrodynamic diameters were measured at 25 °C using a Malvern Nanosizer ZS instrument equipped with a 4 mW He–Ne solid-state laser operating at 633 nm. Back-scattered light was detected at 173°, and the mean particle diameter was calculated from the quadratic fitting of the correlation function over 30 runs of 10 s duration. All measurements were performed in triplicate on very dilute (0.001 w/v %) dispersions containing various NaCl concentrations (no salt and 0.001, 0.50, and 2.0 M) to assess the effect of added salt on the hydrodynamic diameter of the P2VP microgel particles at low pH. Data were collected and analyzed using the Stokes–Einstein equation, which is valid for dilute, spherical, noninteracting particles. It has been shown recently

(18) FitzGerald, P. A.; Dupin, D.; Armes, S. P.; Wanless, E. J. *Soft Matter* **2007**, *3*, 580.

(19) (a) Stöhr, J. *NEXAFS Spectroscopy*; Springer-Verlag: New York, 1992. (b) Dhez, O.; Ade, H.; Urquhart, S. G. *Electron Spectrosc. Relat. Phenom.* **2003**, *128*, 85. (c) Ade, H.; Zhang, X.; Cameron, S.; Costello, C.; Kirz, J.; Williams, S. *Science* **1992**, *258*, 972.

(20) Ade, H.; Hitchcock, A. P. *Polymer* **2008**, *49*, 643.

(21) (a) Lawrence, J. R.; Swerhone, G. D. W.; Leppard, G. G.; Araki, T.; Zhang, X.; West, M. M.; Hitchcock, A. P. *Appl. Environ. Microbiol.* **2003**, *69*, 5543. (b) Toner, B.; Fakra, S.; Villalobos, M.; Warwick, T.; Sposito, G. *Appl. Environ. Microbiol.* **2005**, *71*, 1300.

(22) (a) Koprinarov, I. N.; Hitchcock, A. P.; McCrory, C. T.; Childs, R. F. J. *Phys. Chem. B* **2002**, *106*, 5358. (b) Mitchell, G. E.; Wilson, L. R.; Dineen, M. T.; Urquhart, S. G.; Hayes, F.; Rightor, E. G.; Hitchcock, A. P.; Ade, H. *Macromolecules* **2002**, *35*, 1336. (c) Harton, S. E.; Lüning, J.; Betz, H.; Ade, H. *Macromolecules* **2006**, *39*, 7729. (d) Déjournat, C.; Köhler, K.; Dubois, M.; Sukhorukov, G. B.; Möhwal, H.; Zemb, T.; Guttman, P. *Adv. Mater.* **2007**, *19*, 1331. (e) Tzvetkov, G.; Graf, B.; Fernandes, P.; Fery, A.; Cavalieri, F.; Paradossi, G.; Fink, R. H. *Soft Matter* **2008**, *4*, 510.

(23) Kilcoyne, A. L. D.; Tylliszczak, T.; Steele, W. F.; Fakra, S.; Hitchcock, P.; Franck, K.; Anderson, E.; Harteneck, B.; Rightor, E. G.; Mitchell, G. E.; Hitchcock, A. P.; Yang, L.; Warwick, T.; Ade, H. *J. Synchrotron Radiat.* **2003**, *10*, 125.

(24) Fujii, S.; Armes, S. P.; Araki, T.; Ade, H. *J. Am. Chem. Soc.* **2005**, *127*, 16808.

that dynamic light scattering using the Stokes–Einstein equation should be a valid method for sizing swollen, porous microgel particles that are subject to the dilute solution constraint.²⁵

STXM Characterization of Poly(2-vinylpyridine) Particles

Wet Cell Sample Preparation. A small droplet of an aqueous dispersion of P2VP latex/microgel particles with controlled pH was placed on a 1 mm × 1 mm, 100-nm-thick Si₃N₄ window (Silson Ltd., U.K.), then covered with a second Si₃N₄ window to form a wet cell. The edges of the cell were sealed with a very thin layer of silicone vacuum grease together with small drops of epoxy resin (5 min of curing time). The resulting wet cell had a thickness of about 500 nm to about 1 μm. Care was taken to ensure that no epoxy resin or silicone grease intruded into the cell. This was confirmed by STXM imaging and spectroscopic studies of the assembled wet cell.

Reference Sample Preparation. The neutral P2VP homopolymer reference was prepared by pressing an aqueous slurry of linear P2VP (prepared by the free radical homopolymerization of 2VP in water in the absence of any colloidal stabilizer) onto a Si₃N₄ window. The protonated P2VP reference was prepared by solvent casting an aqueous sulfuric acid solution of P2VP homopolymer at pH 1 onto a Si₃N₄ window. (This protonated P2VP reference was originally prepared using aqueous HCl at pH 1. However, this sample proved to be chemically unstable because the development of a peak at around 398.9 eV due to neutral P2VP was observed during NEXAFS studies, indicating partial loss of volatile HCl. In contrast, sulfuric acid is much less volatile than HCl).

STXM Measurement and Data Processing. STXM measurements were carried out using the STXM polymer instrument at beamline 5.3.2 of the Advanced Light Source (ALS) at Lawrence Berkeley National Laboratory. The transmitted intensity (*I*) of the particles or reference materials was normalized by the transmitted intensity (*I*₀) through Si₃N₄ windows without the particles/materials to yield the optical density OD = −ln(*I*/*I*₀). The effect of the Si₃N₄ membrane on the spectra is thus normalized out. These raw NEXAFS spectra were smoothed, and a linear background was subtracted from each spectrum. The raw transmission images were Fourier filtered to remove periodic noise and then converted to an optical density scale. Image and spectral processing was carried out using the aXis2000 package provided by Adam Hitchcock (available from <http://unicorn.mcmaster.ca/aXis2000.html>), which is coded in Interactive Data Language (IDL) (Research Systems Inc.).

Results and Discussion

The sterically stabilized P2VP latex/microgel particles used in this study were synthesized by free radical copolymerization of 2VP with 1 mol % divinylbenzene (based on 2VP) in the presence of PEGMA in an aqueous solution as described by Dupin et al.^{16c} The number-average particle diameter of the dried P2VP latex particles (Figure 2a) was measured to be 370 ± 20 nm (coefficient of variation (CV), 3%) by scanning electron microscopy (SEM) studies, and the p*K*_a value for the cross-linked P2VP chains was determined by acid titration to be approximately 4.1. Aqueous electrophoresis studies on a dilute aqueous dispersion of these P2VP particles indicated an isoelectric point at approximately pH 6.3, which is in excellent agreement with that reported earlier.^{16c} The milky-white aqueous latex observed at pH 6.5 became noticeably less turbid at pH 3.0 because the refractive index difference between the swollen

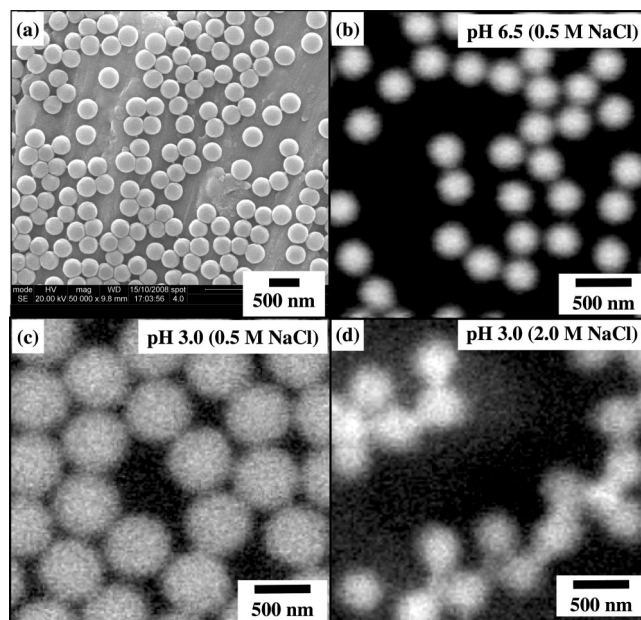


Figure 2. (a) Scanning electron microscopy image of P2VP latex dried at neutral pH. STXM optical density images of aqueous dispersions of P2VP particles (b) in their nonswollen latex state (pH 6.5, 0.5 M NaCl), (c) in their swollen cationic microgel state (pH 3.0, 0.5 M NaCl), and (d) in their salt-induced deswollen microgel state (pH 3.0, 2.0 M NaCl), respectively. Typical STXM imaging times were 5–10 min per image.

microgel particles and the aqueous solution is reduced significantly, leading to much less scattered light. It is perhaps worth emphasizing that linear P2VP latexes (prepared at pH 8.3 in the absence of any DVB cross-linker) simply dissolved in acidic solution to give a viscous aqueous solution: on adjusting the solution pH to 9, the deprotonated P2VP chains precipitated from solution. This control experiment confirmed that cross-linking is essential for the protonated P2VP chains to “remember” their former colloiddally stable latex state.

Detailed DLS studies of the pH-dependent hydrodynamic dimensions of sterically stabilized P2VP particles in dilute aqueous solution at zero salt concentration are summarized in Figure 3. At pH 10, the hydrodynamic (intensity-averaged) latex diameter was approximately 380 nm, which is slightly larger than the number-average diameter of 370 nm estimated from the SEM image shown in Figure 2a. The majority of the pyridine groups become protonated below pH 4.1, which results in electrostatic repulsion between the highly cationic chains. The intensity-averaged diameter of the P2VP microgel particles is around 1400 nm at pH 3.0, which indicates a volumetric swelling factor of approximately 40.

Figure 3 also shows the effect of added salt (0.001, 0.50 and 2.0 M NaCl) on the pH dependence of the P2VP particle diameter as a function of pH at 25 °C. Above pH 4.5, the hydrodynamic diameters are almost constant, and the sterically stabilized particles remain colloiddally stable at each salt concentration. The microgels exhibited a critical latex-to-microgel swelling transition between pH 4.0 and 4.5 at every salt concentration. This corresponds to the p*K*_a value determined for the P2VP microgels by acid titration. The P2VP particles acquire microgel character at low pH because of the protonation of their pyridine residues. The degree of swelling of the microgel particles was suppressed at higher salt concentration: the mean hydrodynamic diameter at pH 3.0 was determined to be 790 and 460 nm in the presence of 0.5 and 2.0 M NaCl, respectively. These diameters are significantly smaller than that for the highly swollen microgel determined in the absence

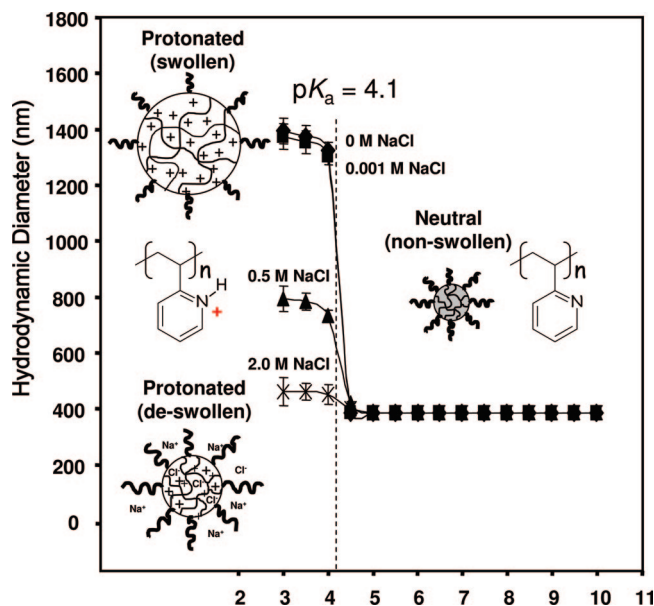


Figure 3. Variation of hydrodynamic diameter with solution pH for lightly cross-linked P2VP particles as a function of added salt: (◆) no salt and (■) 0.001, (▲) 0.5, and (×) 2.0 M NaCl. The error bars for the diameters measured above pH 4.1 are within the data points.

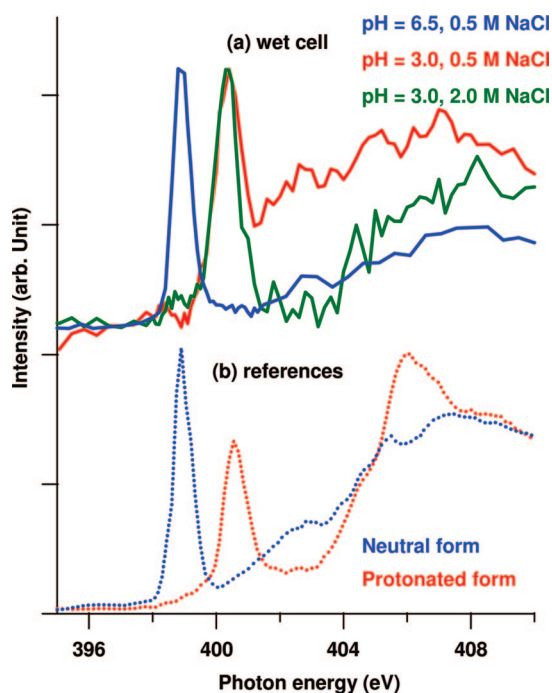


Figure 4. N 1s NEXAFS spectra of (a) P2VP particles in the STXM wet cell at pH 6.5 and 3.0 in the presence of added NaCl and (b) the linear P2VP homopolymer dried in either its neutral or fully protonated state on Si_3N_4 .

of NaCl (~ 1400 nm) as a result of the screening of electrostatic repulsions between the cationic P2VP chains. Removing the electrolyte by dialysis at pH 3 allows the microgel particles to swell reversibly to attain their “zero salt” dimensions.

Both STXM imaging and spectroscopic studies were conducted by focusing on the N 1s core-line signal in NEXAFS. This region was selected because the pH-sensitive chemical environment of the nitrogen atoms is of particular interest for the present system. Figure 4b shows the N 1s NEXAFS spectra obtained for both the neutral and protonated forms of the linear P2VP homopolymer, which was used as a reference material. For neutral P2VP placed

on a Si_3N_4 membrane, the lowest photon energy peak is at 398.9 eV. This is due to the N 1s to π^* transition (i.e., N^0 species) and is in good agreement with the NEXAFS spectra previously reported for both poly(4-vinylpyridine)^{24,26} and also a pyridine multilayer on a metal surface.²⁷ In the spectrum recorded for the protonated cationic P2VP film (cast onto Si_3N_4 from an aqueous H_2SO_4 solution at pH 1), the π^* peak shifts to a significantly higher energy (400.4 eV). This is primarily due to a 1s core-line shift due to reduced screening, indicating that the nitrogen atoms are in their cationic state (i.e., N^+ species).²⁸ Similar changes in N 1s NEXAFS spectra were reported for other cationic polyelectrolytes, such as poly(4-vinylpyridine)^{24,26} and polyaniline.²⁸ Thus, these well-resolved peaks are excellent markers for the protonated and neutral states of the nitrogen atoms in the P2VP chains, and the corresponding two photon energies provide sufficient chemical contrast between the P2VP latex at high pH and the P2VP microgel particles at low pH.

In the presence of very low/zero salt, the swollen microgel diameter exceeds $1\ \mu\text{m}$ at low pH, which is larger than the thickness of the STXM cell. Thus, to minimize the possibility of deformation of the P2VP microgels, STXM images were obtained at 0.5 and 2.0 M NaCl (rather than at zero or 0.001 M NaCl). The STXM optical density image shown in Figure 2b was recorded at 398.9 eV and indicates a number-average particle diameter of 360 ± 15 nm (CV, 3%) for the nonswollen P2VP particles at pH 6.5 in 0.5 M NaCl. Given the relatively small population of particles that were counted, this is in good agreement with the SEM image shown in Figure 2a. The swollen cationic microgels obtained at pH 3.0 in 0.5 M NaCl aqueous solution were imaged at 400.4 eV (Figure 2c). The number-average diameter was estimated to be 630 ± 15 nm (CV, 3%), which is somewhat smaller than the intensity-average diameter of 790 nm in 0.50 M NaCl indicated by DLS. This difference is simply attributed to the effect of polydispersity: DLS is biased toward the larger particles in the size distribution. The STXM images suggest that the swollen microgel particles are well dispersed rather than aggregated. Although approximately micrometer-sized, the swollen cationic P2VP microgels could not be observed using OM, in part because of the inherent resolution of this technique and in part because of the lack of contrast. The deswollen cationic microgels obtained at pH 3.0 in the presence of 2.0 M NaCl (Figure 2d) were also imaged at 400.3 eV. The mean number-average diameter was estimated to be 410 ± 30 nm (CV, 6%), which is again somewhat smaller than the intensity-average diameter of 460 nm reported under the same conditions by DLS. The STXM images also suggest that the salt-induced deswollen microgel particles are well dispersed rather than aggregated.

NEXAFS studies were also conducted on the individual P2VP particles observed in Figures 2 in order to assess their degree of protonation (Figure 4a). The N 1s NEXAFS spectra recorded at both pH 3.0 and 6.5 in the presence of 0.50 M NaCl have sharp peaks at the same photon energies as the corresponding P2VP reference spectra (Figure 4b). Although there are some subtle differences between the spectra obtained for the swollen microgel particles and the protonated P2VP homopolymer reference, there is little or no evidence of neutral nitrogen species (N^0) being

(26) Krishnan, S.; Ward, R. J.; Hexemer, A.; Sohn, K. E.; Lee, K. L.; Angert, E. R.; Fischer, D. A.; Kramer, E. J.; Ober, C. K. *Langmuir* **2006**, *22*, 11255.

(27) (a) Johnson, A. L.; Muettterties, E. L.; Stohr, J.; Sette, F. *J. Phys. Chem.* **1985**, *89*, 4071. (b) Bader, M.; Haase, J.; Frank, K. H.; Puschmann, A.; Otto, A. *Phys. Rev. Lett.* **1986**, *56*, 1921.

(28) (a) Ito, E.; Oji, H.; Araki, T.; Oichi, K.; Ishii, H.; Ouchi, Y.; Ohta, T.; Kosugi, N.; Maruyama, Y.; Naito, T.; Inabe, T.; Seki, K. *J. Am. Chem. Soc.* **1997**, *119*, 6336. (b) Hennig, C.; Hallmeier, K. H.; Szargan, R. *Synth. Met.* **1998**, *92*, 161.

present in either case. Instead, the photon energy peak at ~ 400.4 eV corresponds to cationic nitrogen species (N^+). The N 1s NEXAFS spectrum acquired from the individual microgel particles at pH 3.0 in the presence of 2.0 M NaCl also shows a sharp peak at the same photon energy, which corresponds to that observed for the swollen microgel at the same pH in the presence of 0.50 M NaCl (Figure 4a). This result indicates that the microgels are fully protonated under these conditions, even though these particles were partially deswollen by the high concentration of added salt. As far as we are aware, this is the first direct visualization of the effect of electrolyte screening on microgel dimensions in aqueous solution.

The STXM images shown in Figure 2b–d typically require accumulation times of 5 to 10 min. In principle, given that colloidal particles normally undergo random Brownian motion, this relatively long time scale should render imaging of individual isolated particles impossible. The most likely explanation for this apparent contradiction is that the cationic microgel (or latex) particles are physically adsorbed to the inside walls of the STXM cell. The fact that the particles are probably adsorbed (and hence immobilized) does not detract from the central message of this letter: STXM can be used to image highly swollen microgels

directly in aqueous solution while simultaneously providing useful spectroscopic information (in this case, the degree of protonation of the P2VP chains in the presence of salt).

Conclusions

Scanning transmission X-ray microscopy allows the direct observation of nonsolvated P2VP latex and acid-swollen P2VP microgels in aqueous solution. Moreover, NEXAFS studies confirm that the nitrogen atoms of the microgel particles are completely protonated at low pH. The addition of salt causes partial deswelling of the microgel particles, and direct spectroscopic analysis of individual particles confirms the retention of their cationic character under these conditions. In each case, the observed particle dimensions are consistent with the DLS data, especially when polydispersity effects are taken into consideration.

Acknowledgment. S.P.A. is the recipient of a Royal Society/Wolfson Research Merit Award. EPSRC is thanked for a postdoctoral grant for S.F. (GR/S69276). Work at NCSU is supported by the U.S. Department of Energy (DE-FG02-98ER45737).

LA804212Y